Appl Biochem Biotechnol (2010) 160:665–681
DOI 10.1007/s12010-009-8650-8

The Operable Modeling of Simultaneous Saccharification and Fermentation of Ethanol Production from Cellulose

Jiacheng Shen · Foster A. Agblevor

Received: 14 October 2008 / Accepted: 14 April 2009 /
Published online: 3 May 2009

Abstract An operable batch model of simultaneous saccharification and fermentation (SSF) for ethanol production from cellulose has been developed. The model includes four ordinary differential equations that describe the changes of cellobiose, glucose, yeast, and ethanol concentrations with respect to time. These equations were used to simulate the experimental data of the four main components in the SSF process of ethanol production from microcrystalline cellulose (Avicel PH101). The model parameters at 95% confidence intervals were determined by a MATLAB program based on the batch experimental data of the SSF. Both experimental data and model simulations showed that the cell growth was the rate-controlling step at the initial period in a series of reactions of cellulose to ethanol, and later, the conversion of cellulose to cellobiose controlled the process. The batch model was extended to the continuous and fed-batch operating models. For the continuous operation in the SSF, the ethanol productivities increased with increasing dilution rate, until a maximum value was attained, and rapidly decreased as the dilution rate approached the washout point. The model also predicted a relatively high ethanol mass for the fed-batch operation than the batch operation.

Keywords Simultaneous saccharification and fermentation · Ethanol · Cellulose · Model · Operating mode

Notation

B	Cellobiose concentration (g/l)
B_1	Convertible cellobiose concentration from the reaction r_1 (g/l)
C	Cellulose concentration (g/l)
C_0	Initial cellulose concentration (g/l)
C_1	Cellulose concentration in the feed flow (g/l)

J. Shen (✉)
Center for Environmental Research and Technology, Bourns College of Engineering,
University of California, 1084 Columbia Ave., Riverside, CA 92507, USA
e-mail: jshen@cert.ucr.edu

F. A. Agblevor
Department of Biological Systems Engineering, Virginia Polytechnic Institute and State University,
Blacksburg, VA 24061, USA

D Dilution rate ($=F/V$) (h^{-1})
e Total enzyme concentration (g/l)
e_e Endo-β-1,4-glucanase and exo-β-1,4-cellobiohydrolase concentration (g/l)
$e_e C_{in}^*$ Ineffective complex formed by the enzymes and substrate (g/l)
G Glucose concentration (g/l)
F Feed rate (l/h)
f Proportionality constant (dimensionless)
K_{1B} Inhibitory constant of cellobiose to the endo-β-1,4-glucanase and exo-β-1,4-cellobiohydrolase (g/l)
K_{1G} Inhibitory constant of glucose to the endo-β-1,4-glucanase and exo-β-1,4-cellobiohydrolase (g/l)
K_{2G} Inhibitory constant of glucose to the glycosidase (g/l)
K_G Glucose saturation constant for the microbial growth (g/l)
k_1 Specific rate constant of cellulose hydrolysis to cellobiose (l/(g h))
k_1' Variable associated with enzyme deactivation (h^{-1})
k_2 Specific rate constant of cellobiose hydrolysis to glucose (h^{-1})
k_3 Product formation coefficient associated with cell growth ($=k_3' Y_{G/E}$) (dimensionless)
k_4 Constant ($=k_4' f$) (l/(g h))
k_4' Specific rate constant of enzyme deactivation (l/(g h))
m Maintenance coefficient for endogenous metabolism of the microorganisms (h^{-1})
r_1 Reaction rate from cellulose to cellobiose (g/(l h))
r_2 Reaction rate from cellobiose to glucose (g/(l h))
r_E Reaction rate of ethanol formation (g/(l h))
r_G Reaction rate of glucose consumption (g/(l h))
r_X Reaction rate of cell formation (g/(l h))
t Residence time (h)
V Liquid volume in reactor (l)
X Cell concentration (g/l)
X_0 Initial cell concentration (g/l)
$Y_{G/E}$ Conversion factor of ethanol from glucose (g/g)
Y_{th} Theoretical ethanol yield
$Y_{X/G}$ Yield coefficient of cell mass on the glucose (g/g)
$Y_{X/E}$ Yield coefficient of cell from ethanol (g/g)
μ Specific cell growth rate constant (h^{-1})
μ_m Maximum specific cell growth rate constant (h^{-1})

Superscript
' Overall masses in the culture (g/l)

Introduction

Generally, there are two operating modes for the bioethanol production from lignocellulosic materials: separate hydrolysis and fermentation (SHF) and simultaneous saccharification and fermentation (SSF). SSF has several advantages over the traditional SHF process. SSF has (1) less inhibitory effect of sugars on the enzymatic activities (2), less capital costs (3), and higher ethanol productivity. Some mathematical models of SSF for ethanol production have been proposed [1–5]. The SSF model developed by Philippidis and Hatzis [2,4] included four differential equations to describe change rates of cellulose, cellobiose, glucose, and microorganism concentrations, and an algebraic equation for ethanol

concentration. The model of Philippidis et al. [2] was used by Moon et al. [6] and Pettersson et al. [7] to describe the SSF processes of steam-exploded wood and softwood, respectively. However, a common shortcoming of these studies is that only three (cellobiose, glucose, and ethanol) or two (glucose and ethanol) components in the SSF processes were simulated. The changes in microorganism concentration over time were not simulated. Hence, the models have not been completely verified because the simulation of four sets of data is more difficult than that of three sets of data. In addition, the cellulose concentrations over time in Philippidis and Hatzis's model [4] are needed for the model to work. However, cellulose is a solid, and measuring its concentration in a suspension is often tedious, particularly when cellulose is in biomass. This shortcoming makes the model inoperable. Furthermore, since ethanol is the main product of the SSF process, it will be more convenient if its concentration change is expressed as a differential equation rather than as an algebraic equation in the model to investigate the dynamics of ethanol in the SSF process.

Batch experiment is the main experimental method used in the SSF for ethanol production from lignocellulosic materials. However, the commercial production of ethanol, as a low value and large volume product, must be a continuous operation to be economical. Thus, one of the main tasks of process engineers is to use the data from batch experiments to predict the effect of continuous process on reducing the production cost relative to the batch process. Philippidis and Hatzis [4] extended their batch model to the continuous model. Unfortunately, their continuous model is not complete because the model does not include enzyme addition. In a continuous operation, the enzyme is gradually lost in the outflow. Furthermore, the enzyme deactivation, which was expressed as an exponential function in Philippidis and Hatzis's model [4], also causes a decrease in effective enzyme concentration. Therefore, adding enzyme during continuous operation is necessary. Otherwise, the reaction rate of enzymatic hydrolysis approaches zero with time, and the steady state of the process, which is a basic property of the continuous operation, cannot be achieved.

In these models, there are more than 17 parameters. Some of these parameters, such as inhibitory constants, were determined from independent enzyme experiments in addition to the SSF experiments. For industrial applications, the SSF models with few parameters are more suitable than those representing the detailed fundamental mechanisms because the parameters in a simple model can be determined through an SSF experiment without other additional experiments.

Fed-batch operation has some unique advantages for biochemical experiments and production. For example, to enhance the ethanol concentration in a broth in order to save energy during distillation, a high feedstock concentration (e.g., 10% (*w*/*v*)) is often used in the batch process. However, it was found that in such a high feedstock concentration, the concentrations of components toxic to fermentation microorganisms also were greatly increased. To reduce the inhibitory effect, fed-batch processes are superior to batch processes due to the incremental substrate concentration [8,9]. Another reason against using the batch process is that in a high substrate concentration, the mass transfer between enzyme and substrate is reduced due to the imperfect mixing, resulting in a low rate of enzymatic hydrolysis. There is no published literature on SSF model of fed-batch operation in ethanol production.

In this study, our objectives were (1) to develop simple and operable SSF models for the batch, continuous, and fed-batch processes. The models should have fewer parameters that can be determined by SSF experiments, while the models still represent the main mechanisms of hydrolysis and fermentation; (2) to estimate the model parameters from fitting the data of the four main components in the batch SSF experiments; and (3) to predict the effects of continuous and fed-batch SSF operations based on the parameters obtained from the batch experiments.

Model Development

Batch Operating Mode

Assumptions of the model are that:

1. Cellulose is converted into glucose through cellobiose. Direct conversion of cellulose to glucose is negligible. This assumption was made because it was impossible to distinguish which fraction of glucose was directly or indirectly converted from cellulose in a culture containing cellulase enzymes. This assumption results in the following series of reactions:

$$\text{Cellulose} \xrightarrow{r_1} \text{Cellobiose} \xrightarrow{r_2} \text{Glucose} \tag{1}$$

2. According to the general principle of enzyme feedback inhibition in a series of enzyme reactions, the end product inhibits the first enzyme [10]. In the products catalyzed by a cellulase system, cellobiose and glucose are the products of endo-β-1,4-glucanase, exo-β-1,4-cellobiohydrolase, and glycosidase, respectively. The reaction rates r_1 (g/(l h)) from cellulose to cellobiose and r_2 (g/(l h)) from cellobiose to glucose during the hydrolysis are, respectively, expressed as

$$r_1 = \frac{k_1' C}{1 + G/K_{1G} + B/K_{1B}} \tag{2}$$

$$r_2 = \frac{k_2 B}{1 + G/K_{2G}} \tag{3}$$

Both r_1 and r_2 are enzymatic catalytic reactions. In principle, the catalyst should be not included in a macro-kinetic rate equation because the catalyst takes part in the chemical reaction, but its mass is not changed. However, enzyme deactivation occurs during hydrolysis due to the following catalytic mechanism of cellulase, which mainly consists of endo-β-1,4-glucanase, exo-β-1,4-cellobiohydrolase, and glycosidase: endo-β-1,4-glucanase and exo-β-1,4-cellobiohydrolase are first adsorbed on the surface of insoluble substrate (cellulose) to form the complexes. These may be the effective complex and ineffective complex. The former further produces the cellobiose and free enzyme, and the latter makes endo-β-1,4-glucanase and exo-β-1,4-cellobiohydrolase to lose their activities. Glycosidase catalyzes the cellobiose into glucose in fluid phase. Therefore, the effect of enzyme deactivation can be included in the 'constant' k_1', which can be expressed as the product of the specific rate constant k_1 and enzyme concentration:

$$k_1' = k_1 e \tag{4}$$

Substituting Eq. 4 into Eq. 2 produces

$$r_1 = \frac{k_1 e C}{1 + G/K_{1G} + B/K_{1B}} \tag{5}$$

where B is the cellobiose concentration (g/l), G is the glucose concentration (g/l), C is the cellulose concentration (g/l), e is the enzyme concentration (g/l), k_1' is variable associated with enzyme deactivation (h^{-1}), k_1 is the specific rate constant of cellulose hydrolysis to cellobiose (l/(g h)), k_2 is the specific rate constant of cellobiose hydrolysis to glucose (h^{-1}), K_{1G} and K_{1B} are the inhibitory constants of glucose and cellobiose to the endo-β-1,4-glucanase and exo-β-1,4-cellobiohydrolase (g/l), respectively, K_{2G} is the inhibitory constant of glucose to the glycosidase (g/l), and t is the residence time (h). Because no solid–liquid reaction occurs for the glycosidase in cellulase, glycosidase deactivation can be negligible.

3. Cell growth follows the Monod model. The reaction rates r_X (g/(l h)) and r_G (g/(l h)) of cell and glucose can be, respectively, expressed as

$$r_X = \mu X = \frac{\mu_m XG}{K_G + G} \tag{6}$$

$$r_G = \frac{r_X}{Y_{X/G}} + mX \tag{7}$$

where μ is the specific cell growth rate constant (h^{-1}), μ_m is the maximum specific cell growth rate constant (h^{-1}), m is the maintenance coefficient for endogenous metabolism of the microorganisms (h^{-1}), K_G is the glucose saturation constant for the microbial growth (g/l), X is the cell concentration (g/l), and $Y_{X/G}$ is the yield coefficient of cell mass on the glucose (g/g). In Eq. 6, the cell death is negligible because it was found that there was no great improvement of fitting precision for these equations if the rate constant of cell death was added into Eq. 6.

4. Product (ethanol) formation associated with the cell growth can be represented as

$$\text{Glucose} \xrightarrow{r_X, r_G, r_E} \text{Ethanol} + \text{Cell} + CO_2 \tag{8}$$

The reaction rate r_E (g/(l h)) of ethanol can be expressed as

$$r_E = \frac{k_3' r_X}{Y_{X/E}} = \frac{k_3 r_X}{Y_{X/G}} \tag{9}$$

where $k_3 = k_3' Y_{G/E}$ is the product formation coefficient associated with cell growth (dimensionless), $Y_{G/E}$ is the conversion factor of ethanol from glucose, $Y_{X/E}$, and $Y_{X/G}$ are the yield coefficients of cell from ethanol, and cell from glucose, respectively.

5. Enzyme deactivation is caused by the ineffective adsorption of endo-β-1,4-glucanase and exo-β-1,4-cellobiohydrolase on the solid substrate. This assumption results in the following reaction,

$$C + e_e \xrightarrow{k_4'} e_e C_{in}^* \tag{10}$$

where e_e is the endo-β-1,4-glucanase and exo-β-1,4-cellobiohydrolase concentration (g/l), $e_e C_{in}^*$ is the ineffective complex formed by the enzymes and substrate (g/l), and k_4' is the

specific rate constant of enzyme deactivation (l/(g h)). The ineffective complex formation rate is assumed to be a second order reaction, which can be expressed as [11]

$$\frac{\mathrm{d}e_{\mathrm{e}}C_{\mathrm{in}}^{*}}{\mathrm{d}t} = -\frac{\mathrm{d}e_{\mathrm{e}}}{\mathrm{d}t} = k_4' e_{\mathrm{e}}^2 \tag{11}$$

because the experimental data of enzymatic hydrolysis showed that a second order enzyme deactivation can describe enzymatic hydrolysis better than a first order reaction. In industrial applications, because the total enzyme concentration e (g/l) is often used and the total enzyme concentration is proportional to the endo-β-1,4-glucanase and exo-β-1,4-cellobiohydrolase concentrations, the endo-β-1,4-glucanase and exo-β-1,4-cellobiohydrolase concentrations can be expressed in terms of the total enzyme concentration,

$$e_{\mathrm{e}} = fe \tag{12}$$

where f is the proportionality constant. Hence, Eq. 11 becomes

$$\frac{\mathrm{d}eC_{\mathrm{in}}^{*}}{\mathrm{d}t} = -\frac{\mathrm{d}e}{\mathrm{d}t} = k_4 e^2 \tag{13}$$

where the constant $k_4 = k_4' f$. The integration of Eq. 13 with the boundary conditions $e = e_0$ at $t = 0$ and $e = e$ at $t = t$ is

$$e = \frac{e_0}{1 + k_4 e_0 t} \tag{14}$$

When $t \rightarrow$ infinite, the enzyme concentration approaches zero.

6. Effects of external and internal mass transfers on the enzyme reaction and microorganism metabolic processes can be neglected based on the assumptions that (1) mixing was perfect so that there was no concentration gradient between the substrate and bulk liquid; (2) the cellulose particles were sufficiently small so that there was no concentration gradient in the interior. This assumption implies that the SSF kinetics is only dependent on time, which can be expressed as a series of ordinary differential equations as shown below.

The overall change rate of cellobiose concentration is expressed as

$$\frac{\mathrm{d}B}{\mathrm{d}t} = \frac{r_1}{0.947} - r_2 = \frac{k_1 eC}{0.947(1 + G/K_{1\mathrm{G}} + B/K_{1\mathrm{B}})} - \frac{k_2 B}{1 + G/K_{2\mathrm{G}}} \tag{15}$$

where 0.947 is the conversion factor of two glucan units in cellulose to cellobiose. Equation 15 combined with Eq. 14 produces

$$\frac{\mathrm{d}B}{\mathrm{d}t} = \frac{r_1}{0.947} - r_2 = \left[\frac{k_1 C}{0.947(1 + G/K_{1\mathrm{G}} + B/K_{1\mathrm{B}})}\right]\left(\frac{e_0}{1 + e_0 k_4 t}\right) - \frac{k_2 B}{1 + G/K_{2\mathrm{G}}} \tag{16}$$

The overall change rates of glucose, cell, and ethanol concentrations are, respectively, expressed as

$$\frac{\mathrm{d}G}{\mathrm{d}t} = \frac{r_2}{0.95} - r_{\mathrm{G}} = \frac{k_2 B}{0.95(1 + G/K_{2\mathrm{G}})} - \frac{\mu_{\mathrm{m}} XG}{(K_{\mathrm{G}} + G)Y_{\mathrm{X/G}}} - mX \tag{17}$$

$$\frac{dX}{dt} = \frac{\mu_m XG}{K_G + G} \tag{18}$$

$$\frac{dE}{dt} = \frac{k_3 \mu_m XG}{(K_G + G) Y_{X/G}} \tag{19}$$

where 0.95 is the conversion factor of cellobiose to two glucose molecules.

Equations 16–19 can be used in principle to simulate the concentration changes of cellobiose, glucose, cell mass, and ethanol with respect to time. However, to make the equations operable, the cellulose concentration should be stated in terms of the other soluble concentrations because the measurement of cellulose concentration, as solid particles in suspension, in Eq. 16 is tedious. Assuming negligible by-product formation, the mass balance on cellulose can be expressed in terms of cellobiose, glucose, ethanol, and cell in the culture as follows:

$$C = C_0 - 0.9G - 0.947B - 0.9E/0.511 - 1.137(X - X_0) \tag{20}$$

where C_0 is the initial cellulose concentration (g/l), X_0 is the initial cell concentration (g/l), the constant 0.9 is the conversion factor of a glucan unit in cellulose to glucose, and 0.511 is the inverse conversion factor of glucose to ethanol. The constant 1.137 is the conversion factor of cellulose consumed to produce yeast (gram cellulose per gram dried cell) assuming the molecular formula of the yeast, *Saccharomyces cerevisiae*, to be $CH_{1.74}N_{0.2}O_{0.45}$ during anaerobic fermentation of glucose [12]. Furthermore, it was noted that the cellobiose concentration in our SSF experiments approached zero (Fig. 1). Therefore, the term B/K_{1B} in Eq. 16 can be negligible.Substituting Eq. 20 into Eq. 16 produces

$$\frac{dB}{dt} = \frac{r_1}{0.947} - r_2 = \frac{k_1[C_0 - 0.9G - 0.947B - 0.9E/0.511 - 1.137(X - X_0)]}{0.947(1 + G/K_{1G})} \tag{21}$$

$$\left(\frac{e_0}{1 + k_4 e_0 t}\right) - \frac{k_2 B}{1 + G/K_{2G}}$$

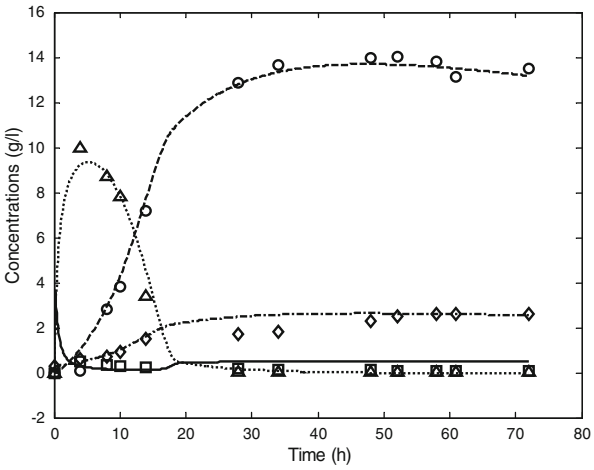

Fig. 1 The experimental points (*symbols*) and simulated curves (*lines*) of cellobiose (*empty square*, *solid line*), glucose (*empty triangle*, *dotted line*), ethanol (*empty circle*, *dashed line*), and cell (*diamond*, *dash-dotted line*) concentrations with time in the batch operation. Conditions: C_0=40 g/l, X_0=0.3 g/l, e_0=4 g/l, and G_0=B_0=E_0=0

Equations 21, 17, 18, and 19 combined with the initial conditions $C=C_0$, $e=e_0$, $X=X_0$, $G=0$, and $B=0$ at time $t=0$ can describe the concentration changes of cellobiose, glucose, cell, and ethanol with respect to time. The parameters k_1, k_2, k_3, k_4, K_G, K_{1G}, K_{2G}, m, and μ_m were determined using a MATLAB fitting program.

Continuous Operating Mode (CSTR)

In the continuous operation, the substrate (cellulose) is continuously fed into the culture at a flow rate F, and the outflow containing ethanol, residual cellulose, cellobiose, glucose, cell, and enzyme exits continuously at the same flow rate F. The overall change rate of cellobiose concentration can be expressed as

$$\frac{dB}{dt} = \frac{r_1}{0.947} - r_2 - DB + DB_1 \tag{22}$$

where $D=F/V$ is the dilution rate (h^{-1}), F is the feed rate (l/h), V is the liquid volume in reactor (l), and B_1 is the convertible cellobiose concentration from the reaction r_1, which is equal to

$$B_1 = \frac{C_1 - C}{0.947} \tag{23}$$

where C is the cellulose concentration in culture, and C_1 is the cellulose concentration (g/1) in the feed flow. Hence, Eq. 22 becomes

$$\frac{dB}{dt} = \frac{r_1}{0.947} - r_2 - DB + \frac{D(C_1 - C)}{0.947} \tag{24}$$

Substituting Eqs. 2, 3, and 20 into Eq. 24 produces

$$\begin{aligned}\frac{dB}{dt} = {} & \frac{k_1 e[C_0 - 0.9G - 0.947B - 0.9E/0.511 - 1.137(X - X_0)]}{0.947(1 + G/K_{1G})} \\ & + \frac{D}{0.947}[C_1 - (C_0 - 0.9G - 0.947B - 0.9E/0.511 - 1.139(X - X_0))] \\ & - \frac{k_2 B}{1 + G/K_{2G}} - DB\end{aligned} \tag{25}$$

Similarly, the overall change rates of glucose, cell, ethanol, and enzyme concentrations are, respectively, expressed as

$$\frac{dG}{dt} = \frac{r_2}{0.95} - r_G - DG = \frac{k_2 B}{0.95(1 + G/K_{2G})} - \frac{\mu_m XG}{(K_G + G)Y_{X/G}} - mX - DG \tag{26}$$

$$\frac{dX}{dt} = \frac{\mu_m XG}{K_G + G} - DX \tag{27}$$

$$\frac{dE}{dt} = \frac{k_5 \mu_m XG}{(K_G + G)Y_{X/G}} - DE \tag{28}$$

$$\frac{de}{dt} = -k_4 e^2 + D(e_0 - e) \tag{29}$$

Fed-Batch Operating Mode

In a fed-batch operation, the substrate (cellulose) is continuously fed into the culture at a flow rate F (usually a constant rate), but no outflow exits from the reactor. In such a situation, the culture volume (V) in the reactor is not constant, but increases at the rate F. The overall change rate dB'/dt (g/h) of cellobiose mass in the culture of fed-batch operation can be expressed as

$$\frac{dB'}{dt} = \frac{Vr_1}{0.947} - Vr_2 + FB_1 \tag{30}$$

$$B_1 = \frac{C_1}{0.947} \tag{31}$$

Substituting Eq. 31 into Eq. 30 produces

$$\frac{dB'}{dt} = \frac{Vr_1}{0.947} - Vr_2 + \frac{FC_1}{0.947} \tag{32}$$

However,

$$\frac{dB'}{dt} = \frac{d(VB)}{dt} = B\frac{dV}{dt} + V\frac{dB}{dt} \tag{33}$$

The change rate dB/dt (g/(l h)) of cellobiose concentration is

$$\frac{dB}{dt} = \frac{r_1}{0.947} - r_2 + \frac{DC_1}{0.947} - DB \tag{34}$$

Substituting Eqs. 2, 3, and 20 into Eq. 34 produces

$$\frac{dB}{dt} = \frac{DC_1}{0.947} - DB + \left\{\left[\frac{k_1 e(C_0 - 0.9G - 0.947B - 0.9E/0.511 - 1.137(X - X_0))}{0.947(1 + G/K_{1G})} - \frac{k_2 B}{1 + G/K_{2G}}\right]\right\} \tag{35}$$

Similarly, the overall change rates (g/(l h)) of glucose, cell, ethanol, and enzyme concentrations can be, respectively, expressed as

$$\frac{dG}{dt} = \left(\frac{r_2}{0.95} - r_G\right) - \frac{GF}{V} = \left[\frac{k_2 B}{0.95(1 + G/K_{2G})} - \frac{\mu_m XG}{Y_{X/G}(K_G + G)} - mX\right] - DG \tag{36}$$

$$\frac{dX}{dt} = \frac{\mu_m XG}{K_G + G} - DX \tag{37}$$

$$\frac{dE}{dt} = \frac{k_5 \mu_m XG}{(K_G + G)Y_{X/G}} - DE \tag{38}$$

$$\frac{de}{dt} = -k_4 e^2 + De_0 - De \tag{39}$$

The change rate of culture volume is expressed as

$$\frac{dV}{dt} = F \tag{40}$$

It is noted that the dilution rate D for a fed-batch operation varies with time, while in the continuous operation D is a constant. The total masses (g/l) of cellobiose (B'), glucose (G'), cell (X'), ethanol (E'), and enzyme (e') in the culture can be calculated by the corresponding concentrations B, G, X, E, and e multiplying the culture volume.

Materials and Methods

Materials

The following substrate and materials were used in the SSF experiments: the microcrystalline cellulose (Avicel PH 101), the Novozymes enzyme NS50052 (Novozymes, North America, Inc. Franklinton, NC, USA), and *S. cerevisiae* (from ATCC). The enzyme activity determined by the filter paper method was 97 FPU/g [13]. The initial enzyme concentration used in the experiments was 4 g/l (enzyme loading used 9.7 FPU/g substrate).

The inoculation medium for *S. cerevisiae* was YM broth, which contained 0.3% yeast extract, 0.3% malt extract, 0.5% peptone, and 1.0% glucose. The fermentation medium contained 0.3% yeast extract, 0.25 g/l $(NH_4)_2HPO_4$, and 0.025 g/l $M_gSO_4{\cdot}7H_2O$.

Experiments of Simultaneous Saccharification and Fermentation

Inoculation of Microorganism

Fresh colonies of *S. cerevisiae* from agar plates were inoculated in 500 ml Erlenmeyer flasks containing 200 ml YM medium with concentration 21 g/l. The cultures were grown in a shaker bath at 35 °C and 200 rpm. The cells were harvested after 18 h, at which time the optical density at 600 nm of the cells in the medium was greater than 0.35 after 10:1 dilution. The cells were centrifuged at 6,000 rpm for 5 min under sterile condition, the supernatants were decanted, and the remaining solid was re-suspended in 50 ml of deionized sterile water. The washing operation was repeated three times. Finally, the cells were stored in 10 ml of deionized sterile water in the refrigerator until the time they were utilized for the fermentation.

Simultaneous Saccharification and Fermentation

The simultaneous saccharification and fermentation experiments were conducted in a 1-l fermenter (B. Braun Biotech International, DCU3). The fermentation medium was composed of 0.5 l citric acid buffer (0.05 M, pH4.8), 20 g Avicel PH 101, and 2.0 g Novozymes enzyme. The medium was initially inoculated with 0.15 g (dried weight) *S. cerevisiae*. The fermentation temperature was maintained at 36 °C, and a pH of 4.8 was maintained by automatic addition of either 2 M hydrochloric acid or 2 M sodium hydroxide solution during the SSF period. The agitation rate was constant at 300 rpm. Two-milliliter

aliquots of the broth were taken periodically and prepared for analysis as described below. The average values of three experiments were reported.

Differential Centrifugation Sedimentation for Separation of Cellulose Particles and Cells from the Broth

Because the Avicel cellulose particles were mixed with the cell mass, direct measurement of cell concentration using the spectrophotometric method was not possible. Thus, the substrate should be first separated from the broth by centrifugation. The aliquot was first centrifuged at 500 rpm for 5 min, which caused only the Avicel particles to settle out because of their higher density than that of the yeast cell. The mixture was decanted, and the supernatant containing the cells and medium was centrifuged again at 6,000 rpm for 5 min. This second centrifugation caused the cells to settle out. The supernatant was then decanted and prepared for high-performance liquid chromatography (HPLC) analysis by filtering through 0.2-μm syringe filter.

Analytical Method

Cell Dry Weight The wet cells from the second centrifugation were dried at 105 °C for 24 h and weighed.

Cellobiose, Glucose, and Ethanol Concentrations The cellobiose, glucose, and ethanol concentrations were measured using Shimadzu 10A HPLC instrument (Shimadzu, Scientific Inc. Kyoto, Japan) equipped with an RI detector, and an auto-sampler (SIL-20AC). A carbohydrate column (7.8×300 mm, BP-100 H^+, 802 Benson Polymeric Inc., Reno, NV, USA) was used for analysis. The column temperature was 60 °C, and the mobile phase was 0.0025 M of sulfuric acid with the flow rate of 0.6 ml/min. The working mode of HPLC was isocratic. The identities of the components were authenticated by comparing their retention times with those of pure compounds (Sigma-Aldrich, St. Louis, MO, USA).

Results and Discussion

The Batch SSF Experiment and Its Simulation

The variations in cellobiose, glucose, ethanol, and cell concentrations with respect to time in the SSF experiment are shown in Fig. 1. The ethanol concentration increased rapidly within the first 30 h, and then leveled off until 48 h. After 48 h, the ethanol concentration slightly decreased probably because of the microbial fermentation of ethanol to form the organic acids. The cellobiose and glucose concentrations peaked in the initial period (Fig. 1), because both cellobiose and glucose were the intermediates in a series of reactions from cellulose to ethanol. It is well known that the intermediate in a series of reactions often has a maximum concentration during the reaction course [14]. Furthermore, because the rate of enzymatic hydrolysis of cellulose at the high enzyme concentration was fast, and the rate of ethanol production at the low cell concentration was slow during this period, both factors caused the accumulations of cellobiose and glucose. It was concluded that the ethanol production in the initial period was controlled by cell growth. After several hours, the cellobiose and glucose concentrations quickly decreased and approached zero because

of the fast cell growth and the decrease in the effective enzyme concentration. The process was then controlled by the enzymatic hydrolysis. Furthermore, the experiment showed that the optimal ethanol productivity for the batch SSF at 48 h was about 0.292 g/(l h), and the maximum ethanol concentration was about 14 g/l, which was equal to a theoretical ethanol yield of 64.4% calculated from the following equation:

$$Y_{\text{th}} = \frac{0.9E}{0.511C_0}100\% \tag{41}$$

This theoretical ethanol yield was similar to other experimental and industrial data [9,15], but lower than 90% stated as the ideal yield [16,17]. This may be because the cellulose in the SSF process had not been completely hydrolyzed due to the suboptimal operating condition for temperature. Another explanation may be that the carbon source required for the yeast growth was not considered in the reaction equation:

$$C_6H_{12}O_6 = 2C_2H_5OH + 2CO_2 \tag{42}$$

which is the basis for the theoretical yield.

The experimental values for the cellobiose, glucose, ethanol, and cell concentrations with respect to residence time were fitted in Eqs. 21, 17, 18, and 19) at the corresponding initial conditions: C_0=40 g/l, X_0=0.3 g/l, G_0=0, B_0=0, e_0=4 g/l, and $Y_{X/G}$=0.515. $Y_{X/S}$ was determined from the experiment on *S. cerevisiae* growth on glucose. The parameters k_1, k_2, k_3, k_4, K_{1G}, K_{2G}, K_G, m, and μ_m in these equations were calculated using the MATLAB Isqnonlin method. These parametric values, their 95% confidence intervals (CI), and the percentages of CIs to the parametric values are listed in Table 1, and the simulated curves are shown in Fig. 1. The percentages of CIs to the parametric values range from 0.16% to 5.7%. From Fig. 1, we can see that the cellobiose concentration with time increased slightly in the later part of the SSF, which may imply that the conversion of cellobiose to glucose declined due to glycosidase deactivation. In Fig. 1, the maximum of the cellobiose concentration was lower than that of the glucose concentration, and the time occurred in the maximum of the cellobiose was earlier than that of the glucose. This implied that the reaction from cellulose to cellobiose is a rate-controlling step because the reaction rate from cellobiose to glucose was faster than that from cellulose to cellobiose. The value k_1e_0 ($0.61\times4=2.44\ h^{-1}$) of r_1 at the initial time is smaller than the rate constants k_2 ($3.20\ h^{-1}$) of r_2, but was greater than the constant $k_3\mu_m$ ($0.535\ h^{-1}$) of r_E (Table 1), which indicated that at the initial time, the process from cellulose to ethanol was controlled by cell growth. However, the enzymatic reaction from cellulose to cellobiose would control the process as the effective enzyme concentration decreased, for example, the enzyme concentration was 0.5 g/l ($k_1e_0=0.305\ h^{-1}<k_3\mu_m<k_2$). The simulated curve of the cell concentrations in Fig. 1 deviated from the experimental data between 20 and 40 h of SSF, compared to the curve deviations from the other experimental points beyond the range between 20 and 40 h. The

Table 1 The parametric values, confidence intervals, and percentages of CIs to values.

	Parameter								
	k_1 (l/(g h))	k_2 (h^{-1})	k_3 (–)	k_4 (l/(g h))	K_{1G} (g/l)	K_{2G} (g/l)	K_G (g/l)	m (h^{-1})	μ_m (h^{-1})
Value	0.6096	3.202	3.024	0.0997	0.1768	16.25	3.399	0.6420	0.1768
CI (±)	0.0281	0.0259	0.1723	0.0056	0.0091	0.0479	0.0073	0.0010	0.0006
%	4.6	0.81	5.7	5.6	5.1	0.29	0.21	0.16	0.34

cell concentrations in the simulated curve between 20 and 40 h had fast increase, while the experimental points had a more linear pattern. The deviation is probably because Eq. 6 is based on the first-order kinetics for cell concentration (μX), which implies an exponential growth of cells in the presence of sufficient growth-limiting substrate. However, the cell growth in the SSF process was limited because of no sufficient sugar supply from the low reaction rate of enzymatic hydrolysis for cellulose. Therefore, the experimental cell growth was slower than the exponential growth expected in theory.

Simulation of Continuous Operation

The variations in glucose, cell, and ethanol concentrations over time at various dilution rates in the continuous operation are shown in Fig. 2. From these graphs, we can see that the model indicates a basic property of the continuous operation: the concentrations of the three components approached the constant values at the steady state as time increased. When the dilution rate was increased, the time to reach the steady state of the system increased. However, when the dilution rate approached the washout point (D=0.08 h^{-1}), the steady state of the system immediately reached the point at which both the cell and ethanol concentrations were very low. At the steady state, the highest ethanol concentration was about 12.2 g/l at the dilution rate 0.01 h^{-1} (Fig. 2c). This value was slightly lower than that in the batch experiment (14 g/l) because (1) this highest ethanol concentration was dependent on the dilution rate. The smaller the dilution rate, the higher the ethanol concentration. (2) The cellulose concentration (C_1 20 g/l) in the feed flow was lower than that in the batch experiment (C_0 40 g/l). Figure 3 shows the glucose, cell, and ethanol concentrations as well as productivity (DE) at the steady state for various dilution rates.

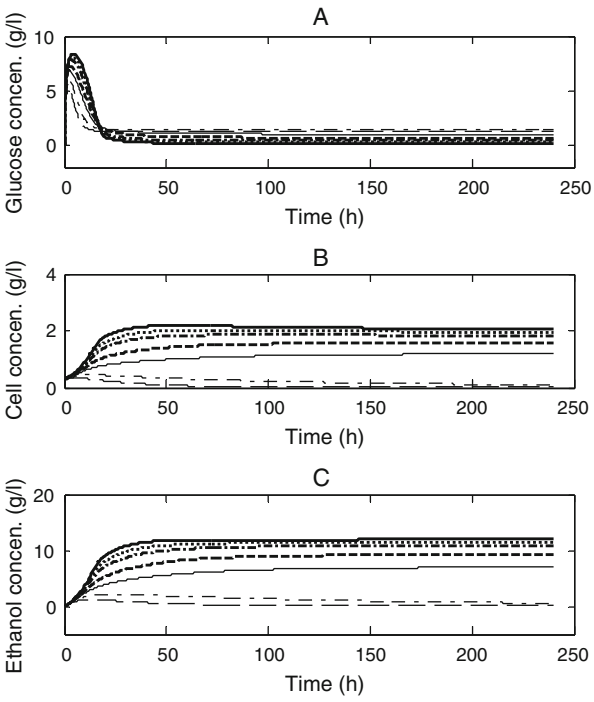

Fig. 2 The simulated glucose (**a**), cell (**b**), and ethanol (**c**) concentration curves (*lines*) with time at eight dilution rates: 0.01 h^{-1} (*thick, solid line*), 0.015 h^{-1} (*thick*, *dotted line*), 0.02 h^{-1} (*thick*, *dash-dotted line*), 0.03 h^{-1} (*thick*, *dashed line*), 0.04 h^{-1} (*fine*, *solid line*), 0.05 h^{-1} (*fine*, *dotted line*), 0.06 h^{-1} (*fine*, *dash-dotted line*), and 0.08 h^{-1} (*fine*, *dashed line*) in the continuous operation. Conditions: C_0=40 g/l, C_1=20 g/l, X_0=0.3 g/l, e_0=4 g/l, e_1=1 g/l, and G_0=B_0=E_0=0

When the dilution rate was increased, the ethanol and cell concentrations decreased, whereas the glucose had a maximum concentration at the dilution rate 0.06 h^{-1}. The ethanol productivity first increased with increased dilution rate until a maximum value (about 0.3 g/(l h)) at a dilution rate of 0.04 h^{-1}, and quickly decreased to zero at a washout state. These observations about ethanol, cell, and productivity showed that the general principle of chemostat operation is applicable to the complicated situation of SSF [18,19]. It should point out that the glucose was an intermediate rather than an initial reactant. Therefore, its concentration did not decrease monotonically with increasing the dilution rate. On the other hand, it also should point out that the extrapolating description of continuous SSF operation based on the batch model parameters only is an estimation of continuous SSF operation from an engineering view rather than an accurate description.

Simulation of Fed-Batch Operation

The variations in the concentrations of glucose, cell, and ethanol with time at the three feed flow rates (0.01, 0.02, and 0.03 l/h) in the fed-batch operation are shown in Fig. 4 (the initial culture volume V_0 1 l, and the cellulose concentration in the feed rate C_1 20 g/l). The corresponding variations of masses with time are presented in Fig. 5. The ethanol and cell concentrations quickly increased before 20 h. After 25 h, the glucose and ethanol concentrations at the three flow rates were almost same (Fig. 4a, c), but there was a slight difference in cell concentrations (Fig. 4b), both of which resulted from the dilution effect of increasing the culture volume. Furthermore, the cell, ethanol, and glucose concentrations at the three feed flow rates were approximately constant after 30 h (Fig. 4). This observation showed that the process achieved a quasi-steady state for the fed-batch operation when the substrate concentration in the feed flow was much greater than that in the culture [20]. It is interesting to note that the cell and ethanol masses in the culture for the fed-batch operation

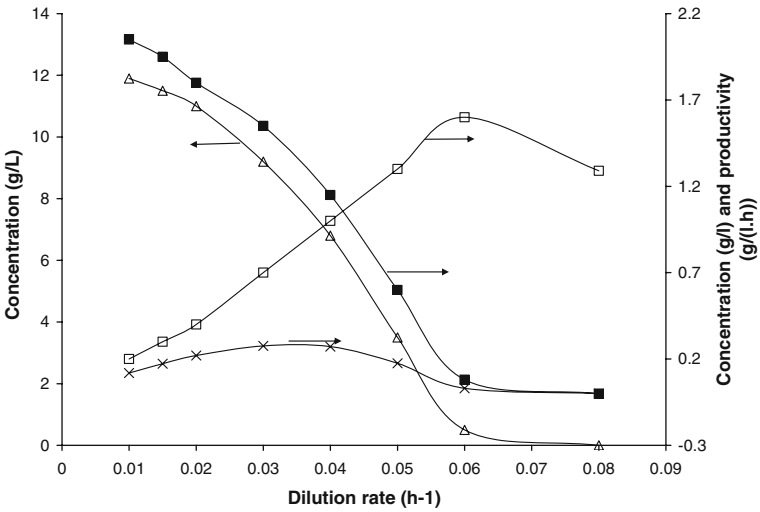

Fig. 3 The glucose, cell, and ethanol concentrations and productivity with dilution rate in the continuous operation. Glucose (*empty square*), cell (*filled square*), ethanol (*empty triangle*), and productivity (*multiplication symbol*). Conditions: C_0=40 g/l, C_1=20 g/l, X_0=0.3 g/l, e_0=4 g/l, e_1=1 g/l, and $G_0=B_0=E_0=0$

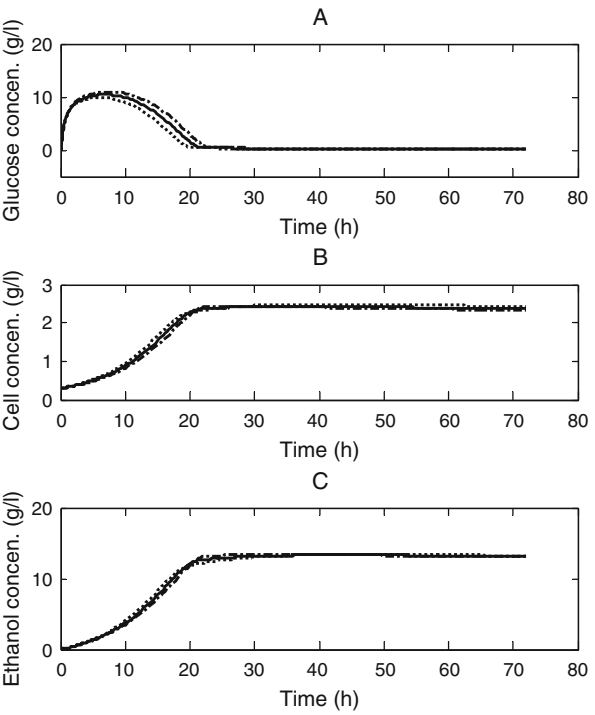

Fig. 4 The simulated glucose (**a**), cell (**b**), and ethanol (**c**) concentration curves (*lines*) with time at three flow rates: 0.01 l/h (*dotted line*), 0.02 l/h (*solid line*), and 0.03 h/l (*dash-dotted line*) in the fed-batch operation. Conditions: C_0=40 g/l, C_1=20 g/l, e_0=4 g/l, e_1=1 g/l, X_0=0.3 g/l, V_0=1 l, and $G_0=B_0=E_0=0$

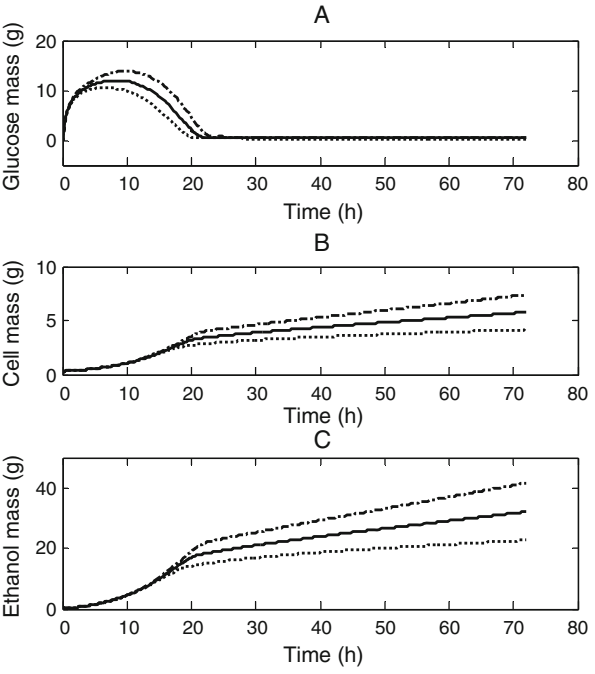

Fig. 5 The simulated glucose (**a**), cell (**b**), and ethanol (**c**) mass curves (*lines*) with time at three flow rates: 0.01 l/h (*dotted line*), 0.02 l/h (*solid line*), and 0.03 h/l (*dash-dotted line*) in the fed-batch operation. Conditions the same as Fig. 4

greatly increased, for example, about 7.5 and 42 g for the flow rate 0.03 l/h, respectively, compared to the cell mess of 2.2 g and the ethanol mass of 14 g in the batch experiment.

Conclusions

The proposed model of the SSF process, which includes the four ordinary differential equations for the description of the changes of cellobiose, glucose, microorganism, and ethanol concentrations with respect to time, can be used to fit the experimental data for the four main components in the SSF process of ethanol production without additional experiments. The predicted values of the model are in agreement with the experimental points of four components of the batch SSF operation. Analysis of the rate constants of the batch model shows that the SSF process of ethanol production from cellulose is controlled by cell growth in the initial period, and then is controlled by the reaction from cellulose to cellobiose. The extended models for the continuous and fed-batch operations were also developed based on the batch model. Both models can be used to predict the dynamics of the continuous and fed-batch SSF operations of ethanol production based on the model parameters obtained from the batch experiments. The simulated fed-batch operation produced much better effect on ethanol production than the batch operation. The simulation also showed that there was an optimal dilution rate for the maximum productivity of ethanol production in the continuous SSF operating process. These models provide estimations for continuous and fed-batch SSF operations from batch experiments.

Acknowledgments The authors acknowledge the National Science Foundation (NSF) under contract No. 0420577 and Xethanol Inc. for providing financial support for this project.

References

1. Philippidis, G. P., Spindler, D. D., & Wyman, C. E. (1992). *Applied Biochemistry and Biotechnology, 34–35*, 543–556. doi:10.1007/BF02920577.
2. Philippidis, G. P., Smith, T. K., & Wyman, C. E. (1993). *Biotechnology and Bioengineering, 41*(9), 846–853. doi:10.1002/bit.260410903.
3. South, C. R., Hogsett, D. A. L., & Lynd, L. R. (1995). *Enzyme and Microbial Technology, 17*(9), 797–803. doi:10.1016/0141-0229(94)00016-K.
4. Philippidis, G. P., & Hatzis, C. (1997). *Biotechnology Progress, 13*(3), 222–231. doi:10.1021/bp970017u.
5. Shin, D., Yoo, A., Kim, S. W., & Yang, D. R. (2006). *Journal of Microbiology and Biotechnology, 16*(9), 1355–1361.
6. Moon, H., Kim, J. S., Oh, K. K., Kim, S. W., & Hong, S. I. (2001). *Journal of Microbiology and Biotechnology, 4*, 598–606.
7. Pettersson, P. O., Eklund, R., & Zacchi, G. (2002). *Applied Biochemistry and Biotechnology, 98*, 733–746. doi:10.1385/ABAB:98-100:1-9:733.
8. Rudolf, A., Alkasrawi, M., Zacchi, G., & Liden, G. (2005). *Enzyme and Microbial Technology, 37*(2), 195–204. doi:10.1016/j.enzmictec.2005.02.013.
9. Zhu, S. D., Wu, Y. X., Zhao, Y. F., Tu, S. Y., & Xue, Y. P. (2006). *Chemical Engineering Communications, 193*(5), 639–648. doi:10.1080/00986440500351966.
10. Lehninger, A. L., Nelson, D. L., & Cox, M. M. (1993). *Principles of biochemistry* (2nd ed., p. 229). New York: Worth.
11. Shen, J. C., & Agblevor, F. A. (2008). *Biochemical Engineering Journal, 41*, 241–250. doi:10.1016/j.bej.2008.05.001.

12. Shuler, M. L., & Kargi, F. (2002). *Bioprocess engineering* (2nd ed., p. 217). New York: Prentice Hall.
13. Ghose, T. K. (1987). *Pure and Applied Chemistry, 59*(2), 257–268. doi:10.1351/pac198759020257.
14. Levenspiel, O. (1999). *Chemical reaction engineering* (3rd ed., p. 171). New York: Wiley.
15. Kosaric, N., & Vardar-Sukan, F. (2001). Potential source of energy and chemical products. In M. Roehr (Ed.), *Biotechnology of ethanol: Classical and future applications* (p. 180). New York: Wiley.
16. Ohgren, K., Bura, R., Lesnicki, G., Saddler, J., & Zacchi, G. (2007). *Process Biochemistry, 42*(5), 834–839. doi:10.1016/j.procbio.2007.02.003.
17. Glazer, A. N., & Nikaido, H. (1995). *Microbial biotechnology* (p. 366). New York: W. H. Freedom and Company.
18. Blanch, H. W., & Clark, D. S. (1996). *Biochemical engineering* (p. 290). New York, NY: Marcel Dekker.
19. Stanburg, P. F., Whitaker, A., & Hall, S. J. (1995). *Principles of fermentation technology* (2nd ed., p. 23). Elsevier: Amsterdam.
20. Pirt, S. J. (1979). Fed-batch culture of microbes. *Annals of the New York Academy of Sciences, 326*, 119–125. doi:10.1111/j.1749-6632.1979.tb14156.x.